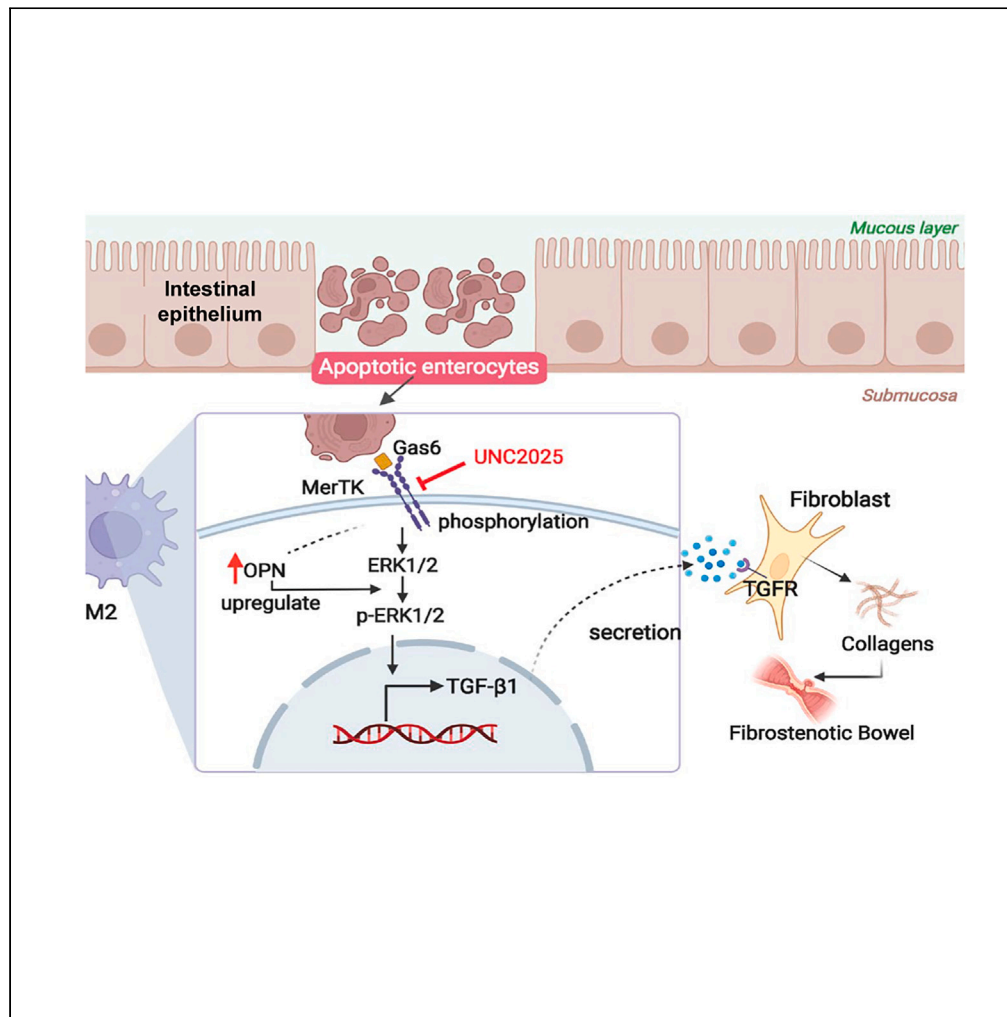


Article

Osteopontin regulation of MerTK⁺ macrophages promotes Crohn's disease intestinal fibrosis



Juanhan Liu,
Wenbin Gong,
Peizhao Liu, ...,
Xiuwen Wu, Yun
Zhao, Jianan Ren

wuxiuwen@nju.edu.cn (X.W.)
zhaoyun056@gmail.co (Y.Z.)
jiananr@nju.edu.cn (J.R.)

Highlights

The etiology of intestinal fibrosis in Crohn's disease remains elusive

This study demonstrates a profibrotic pathway in intestinal MerTK⁺ macrophages

Osteopontin upregulates MerTK pathway, resulting in TGF-β1 production

This study provides a promising therapeutic target for intestinal fibrosis



Article

Osteopontin regulation of MerTK⁺ macrophages promotes Crohn's disease intestinal fibrosis

Juanhan Liu,¹ Wenbin Gong,² Peizhao Liu,¹ Yangguang Li,¹ Haiyang Jiang,³ Cunxia Wu,³ Xiuwen Wu,^{1,*} Yun Zhao,^{3,*} and Jianan Ren^{1,4,*}

SUMMARY

The pathogenesis of intestinal fibrosis in Crohn's disease (CD) remains unclear. Mer receptor tyrosine kinase (MerTK) is an immunosuppressive protein specifically expressed in macrophages. Osteopontin (OPN), also known as secreted phosphoprotein 1, contributes to inflammation and wound repair. This study investigates the potential profibrotic pathway in MerTK⁺ macrophages in order to provide a possible therapeutic target for intestinal fibrosis. MerTK expression in the inflamed and stenotic bowels was evaluated. The MerTK/ERK/TGF- β 1 pathway was overactivated in the fibrotic intestinal tissues of patients with CD. This pathway was induced by epithelial cell apoptosis, resulting in activated fibroblasts with increased TGF- β 1 secretion. OPN upregulated TGF production by altering ERK1/2 phosphorylation, as evidenced by OPN or MerTK knockdown and OPN overexpression *in vitro*. MerTK inhibitor UNC2025 alleviated intestinal fibrosis in mouse colitis models, suggesting a potential therapeutic target for intestinal fibrosis in patients with CD.

INTRODUCTION

Intestinal fibrosis (IF) is a common and severe complication of Crohn's disease (CD). With the rapidly rising incidence of inflammatory bowel disease (IBD) in Asia,¹ IF has become a burden, notably for individuals with CD. Due to the IF's unclear etiology, current medical therapy choices are limited. Notably, refractory clinical obstruction always necessitates endoscopic or surgical intervention. Although chronic inflammation was originally thought to be responsible for the intricate pathogenesis of stricture formation, new evidence for noninflammatory contributors to stricture formation has emerged, suggesting an intricate interplay between cellular, molecular, and other potential hosts/environmental factors. Therefore, more in depth understanding of the pathogenesis and thus new therapeutic targets in IF are desperately needed.

Although various factors may contribute to fibrosis development, inflammation plays a primary role in this complex process, as no fibrotic lesions have been identified in areas other than the inflammatory bowel, even in cases of recurrent fibrosis following enterectomy.² After surgical excision of the lesion, fibrosis tends to recur away from the anastomotic sites.³ Notably, current research has demonstrated that anti-inflammatory agents are ineffective in preventing, relieving, or treating fibrosis in colitis, suggesting that antifibrotic therapy requires reconsideration in a novel, inflammation-independent manner that is not limited to inflammation inhibition. A TNBS (chronic trinitrobenzene-sulfonic acid) model of inflammation-induced colonic fibrosis⁴ exhibited an early increase in inflammation-related genes followed by a rapid decline, suggesting that overactive repair, after reduction in acute inflammation, significantly contributes to fibrotic disease progression.

Currently, transforming growth factor (TGF)- β 1 is the most important profibrotic factor. TGF- β and its receptors prefer to localize to lamina propria cells, especially close to the luminal surface, a site enriched with diverse immune cells that appears to be upregulated in biopsy specimens and myofibroblasts from areas of intestinal stricture.⁵ Because systemic targeting of Smad3 may impair host T cell immunity,⁶ determining a target to partly inhibit the TGF pathway for treating fibrotic lesions is necessary. Numerous upstream factors, such as highly plastic macrophages, are implicated in TGF pathway activation and play a dual role in tissue damage and repair. The TAM family, comprising Tyro3, AXL, and Mer receptor tyrosine kinase (MerTK), and its cognate glycoprotein ligands (growth arrest-specific (Gas)6 and protein S) are important tissue homeostasis and inflammation regulators.⁷ TAMs are immunosuppressive regulators that may help resolve inflammation and repair damaged tissue after conditions including acute liver failure⁸ and myocardial infarction,⁹ suggesting their ability to induce overactive repair and fibrosis when inflammatory diseases persist, such as in IBD. Unlike ulcerative colitis (UC), transmural inflammation in CD renders clinical obstruction more common, although UC development may still involve fibrotic pathological changes. Pathological fibrosis is observed in almost all UC colectomy specimens.¹⁰ Therefore, chronic inflammation should be largely considered for the effective treatment of fibrosis, especially the immunosuppressive factors that predominate when inflammation becomes chronic.

¹Department of General Surgery, Research Institute of General Surgery, Jinling Hospital, Affiliated Hospital of Medical School, Nanjing University, Nanjing, China

²Department of General Surgery, School of Medicine, Southeast University, Nanjing, China

³Department of General Surgery, BenQ Medical Center, Nanjing Medical School, Nanjing, China

⁴Lead contact

*Correspondence: wuxiuwen@nju.edu.cn (X.W.), zhaoyun056@gmail.co (Y.Z.), jiananr@nju.edu.cn (J.R.)

<https://doi.org/10.1016/j.isci.2024.110226>



MerTK significantly regulates macrophage M1/M2 polarization and inflammation in the brain,¹¹ liver,¹² lung,¹³ heart,¹⁴ and kidney.¹⁵ Gas6, a typical ligand for the TAM family, markedly modulates the inflammation-fibrosis interplay.¹⁶ Recent studies have focused on its possible function in fibrotic disease, such as liver fibrosis in nonalcoholic steatohepatitis,¹⁷ and Ig4-related diseases.¹⁸ However, Gas6's specific mechanism remains unclear, especially in the gut. Upon activation, as a receptor tyrosine kinase (RTK), the intracellular tyrosine kinase domain (carboxyl terminal) is responsible for downstream cytoplasmic signaling. For instance, the phosphorylated sites of MerTK could bind to Src homology (SH)2 domains, thus recruiting SH2-domain-containing proteins and activating related pathways, such as the suppressor of cytokine signaling, growth factor receptor-bound protein 2, and mitogen-activating protein kinase (MAPK).¹⁹ Notably, the nature of widespread recruitment makes it difficult to identify the pathways that work in different disease states. In addition, the role of MerTK in the development of IBD remains unclarified. ADAM17 (ADAM metalloproteinase domain 17), also known as a tumor necrosis factor (TNF) α -converting enzyme, which belongs to the disintegrin and metalloproteinase family, can hydrolyze the extracellular domain of MerTK. Once ADAM17 sheds the ectodomain structure of MerTK, generating soluble forms (sMerTK), MerTK loses its affinity for ligands, fails to be a decoy receptor, and stops exerting its biological effects. ADAM17 is ubiquitously expressed in the human colon and is increased in IBD (both CD and UC),²⁰ and its activity is associated with disease development. Blaydon et al. identified a loss-of-function mutation in ADAM17 as the cause of inflammatory skin and bowel disease in two of three children born to consanguineous parents,²¹ and later reports on ADAM17 revealed its relation to very-early-onset IBD.²² These studies indirectly indicated that the TAM family and IBD may be associated. The present study explored the direct role of MerTK in IF and identified a potential therapeutic target for CD.

In addition to investigating the fibrosis-related MerTK/extracellular signal-regulated kinase (ERK)/TGF- β 1 pathway in IF development, we focused on what activates MerTK in CD and the possible factors that regulate the whole signaling pathway, given that ERK is universally activated in CD.²³ MerTK is inextricably linked to efferocytosis, the macrophage-dominated process of clearing apoptotic cells mediated by the GAS6/MerTK system. Notably, apoptotic cell phagocytosis can induce alternatively activated macrophage growth to repair tissue injury.²⁴ Enterocyte apoptosis can promote IF in CD mediated by CD36/CD36R and ERK1/2 activation.²⁵ ERK, a MAPK family member, is a typical downstream signal of MerTK phosphorylation. These studies revealed that apoptotic cells may be a source of activated MerTK⁺ macrophages; thus, we hypothesize that apoptotic enterocytes activate the MerTK pathway in intestinal macrophages and promote fibrosis in CD.

Shen et al. reported that osteopontin (OPN) is essential for CD11c⁺ microglial cell stability, phagocytosis, and proliferation. Significantly decreased homing of CD11c⁺ macrophages to the brain and defects in macrophage-related function were observed in OPN-deficient mice,²⁶ suggesting that OPN plays an irreplaceable role in maintaining macrophage functions. Although OPN was first identified as a cytokine with proinflammatory activity, its prohealing or potentially profibrotic function has eventually been identified. Morse et al. reported the colocalization of MerTK and OPN in the profibrotic macrophages of patients with idiopathic pulmonary fibrosis (IPF).²⁷ They defined a proliferative pulmonary MerTK⁺ macrophage subset that expresses highly upregulated OPN and used causal modeling to support its profibrotic role in lung fibrosis. OPN activates fibroblasts *in vitro* as a form of exocytosis, and OPN-deficient macrophages produce reduced TGF- β levels in dermal fibrosis.²⁸ Based on these studies, we further investigated whether OPN and MerTK interact in macrophages.

This study investigates the role of MerTK in IF development in CD, determines critical events in activating the MerTK pathway, identifies regulatory factors for this pathway in macrophages, and determines whether UNC2025, a MerTK-targeting inhibitor, can attenuate IF in experimental animal models.

RESULTS

Increased MerTK expression in the fibrostenotic bowel and decreased expression in the inflamed area of CD

To investigate whether MerTK is associated with CD development, its protein expression and transcriptional levels were evaluated in stenotic, inflamed, and nonstenotic, noninflamed bowel biopsies from patients with CD (Figures 1A–1C). Consistent with clinical bowel stricture, MerTK expression (both transcriptional and protein levels) was significantly higher in the stenotic bowel and markedly lower in the inflamed area compared to the nonstenotic area. Immunohistochemical staining of MerTK in human bowel samples corroborated the western blot and qPCR analysis results (Figure 1B). Table S1 lists the detailed clinical characteristics of the patients. All suspected stenotic segments of the intestine were preliminarily confirmed by preoperative gastrointestinal radiography and intraoperative biopsy specimen observation by a surgeon. Representative Masson trichrome staining confirmed the increased deposition of collagen in the stenotic intestine (Figure S1A). In the gut, types I, III, IV, and V collagens predominate, and type I, III, and IV are highly increased in the fibrotic intestines of patients with CD.²⁹ Consistent with these reports, types I, III, and IV collagens demonstrated increased transcription in the stenotic specimens (Figure 1C). In addition, a significantly decreased transcriptional level of type IV collagen, which was abundantly expressed in the basement membrane,²⁹ was observed in the inflamed area, which may be attributed to the damage to the basement membrane caused by transmural inflammation because inflammation is restricted to the mucosa or submucosa in UC but extends throughout the entire thickness of the small or large bowel wall in CD. Immunohistochemical staining of collagen (COL1A1/COL3A1) in fibrotic or control human specimens (Figure S1B) revealed increased deposition of types I and III collagen in the stenotic area. In addition, the staining images showed that, closer to the subepithelial area, the difference in staining for COL1A1/COL3A1 became even more pronounced, suggesting that changes in collagen deposition in the lamina propria were more pronounced in these patients. The transcription level of TGF- β 1, the most important profibrotic factor in CD, increased in the stenotic area but did not significantly change in the inflamed area (Figures 1A and 1C). Colocalization of MerTK and CD206, a typical marker of anti-inflammatory M2 macrophages, was found in human specimens, even in the control group (Figure 1D). Not all MerTK colocalized with CD206, suggesting that MerTK⁺ macrophages cannot be considered M2-type macrophages. In addition, the CD206-marking green fluorescence signal was much less colocalized with MerTK in the control and inflamed human samples

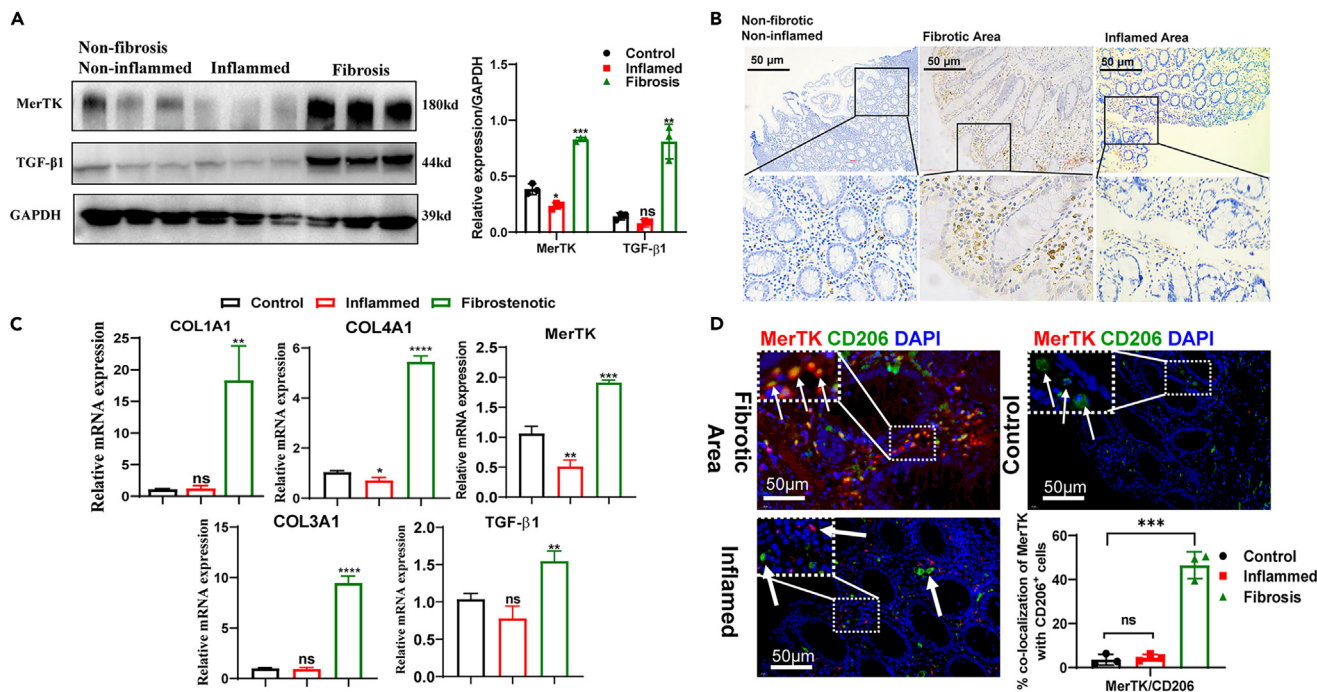


Figure 1. MerTK expression increased in the fibrostenotic bowel and decreased in the inflamed bowel area in patients with CD

(A) Western blotting and quantitative grayscale analysis (compared to the control group) of MerTK and TGF- β 1 protein expression in the resected intestinal mucosal specimen.

(B) Immunohistochemical staining of MerTK in bowel specimens.

(C) qPCR evaluation of MerTK, TGF- β 1, COL1A1, COL3A1, and COL4A1 levels in bowel specimens.

(D) Immunofluorescence staining and colocalization of MerTK and CD206 in human specimens. The colocalization percentage was analyzed by ImageJ, and statistical analysis was performed in GraphPad Prism (compared to the control group).

(colocalization percentage between MerTK and CD206: $3.56\% \pm 2.51\%$ [mean \pm SD, control], $4.54\% \pm 1.53\%$ [mean \pm SD, inflamed], and $46.46\% \pm 6.09\%$ [mean \pm SD, fibrosis]). In the inflamed tissue, the fluorescence signal of CD206 increased, whereas the red fluorescence signal of MerTK did not (Figure 1D). During fibrosis progression, an unknown stimulus upregulates MerTK irrespective of CD206 expression, revealing M2-biased polarization.

These results indicate that MerTK expression on CD206⁺ macrophages occur with the progression of CD-related diseases (Figure 1D). While MerTK positively correlates with stenotic CD development, it plays a restorative role and was inhibited or activated by various factors in the intestinal microenvironment.

Apoptotic enterocytes induced MerTK-ERK1/2 activation in macrophages and increased TGF- β 1 secretion

We focused on changes in MerTK in the stenotic bowel and attempted to explain the increased expression. Based on recent reports about apoptosis-induced fibrosis and our observation in human samples that TGF- β 1 transcription was significantly increased in the stenotic area, we hypothesized that apoptosis of intestinal epithelial cells would activate the MerTK/ERK pathway and eventually result in TGF- β 1 secretion. The apoptosis level was detected in human samples by immunofluorescent staining of cleaved-caspase3 (Figure 2A). Excessive apoptotic cells were observed in the stenotic intestinal mucosa, and fluorescence was enriched in the epithelial cells, which supported enterocyte apoptosis. Multiple regions of fluorescent signals were captured in the inflamed tissue, indicating that apoptosis occurred across the entire thickness of the intestinal mucosa in response to inflammatory injury. To further explore the effect of apoptotic enterocytes on macrophages, we incubated RAW 264.7 cells with apoptotic CT26 cells (induced by UV irradiation) for 1 h (Figure S1C). Western blotting for caspase 3 and cleaved-caspase 3 was used to verify CT26 apoptosis (Figure 2B). The MerTK transcription and phosphorylation levels increased, with no obvious change in the protein level of the total MerTK (Figures 2C and 2D). Recent studies have confirmed the anti-inflammatory function of Gas6, a ligand for MerTK, in macrophages. Furthermore, it has been established that Gas6 relies on its TAM ligand on macrophages to exert its function. Therefore, Gas6 was utilized as a MerTK inducer in MerTK-related *in vitro* investigations. Gas6 exhibited a slight increase in transcription and activated MerTK in other macrophages, resulting in an amplified MerTK signaling pathway. The longer UV irradiation reduced this increasing trend. A higher load or longer duration of UV exposure also led to cell death, rather than just early apoptosis, possibly causing elevated inflammation that was not effectively and rapidly cleared by phagocytes. When MerTK was phosphorylated, ERK1/2 was also activated (Figure 2B), initiating the production of downstream TGF- β 1.

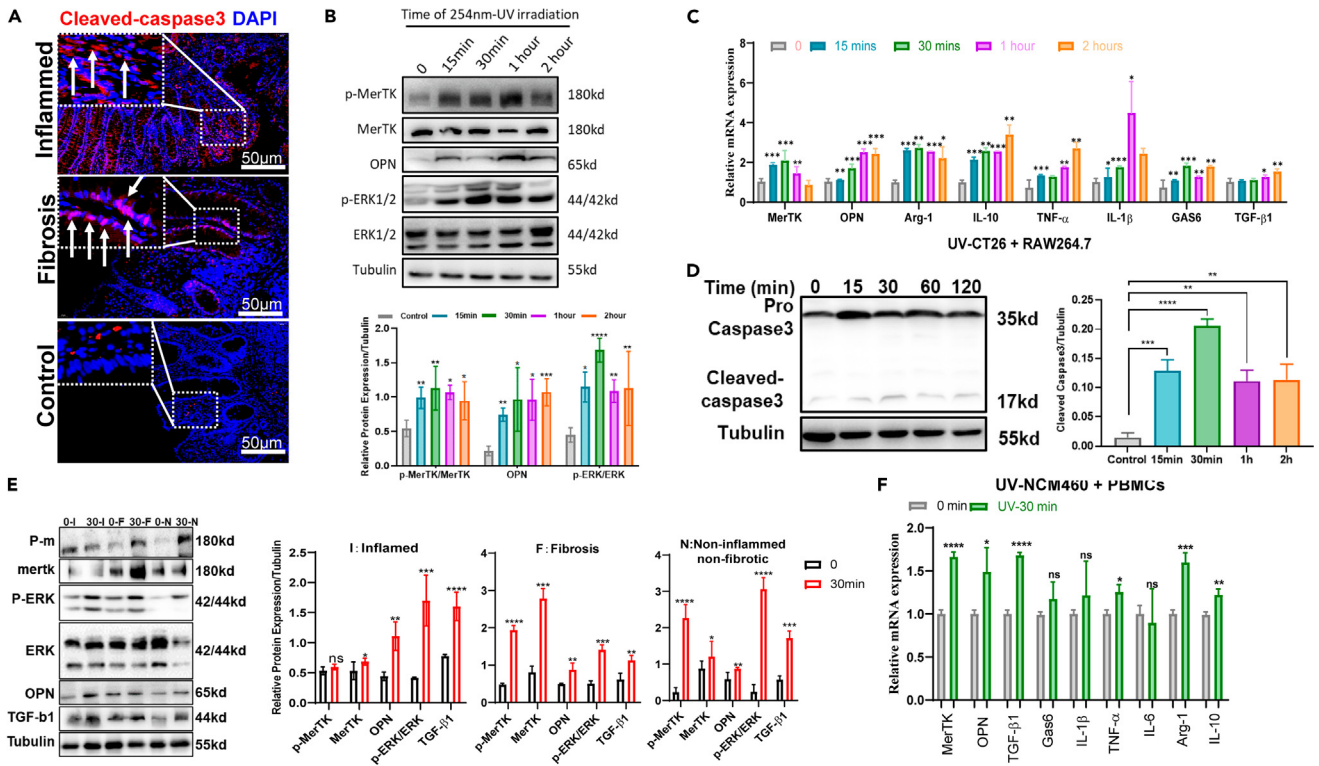


Figure 2. Apoptotic intestinal epithelial cells induced activation of MerTK-ERK1/2 pathway in macrophages and M2-biased polarization

(A) immunofluorescence staining of cleaved-caspase 3 in human specimens.

(B) change in the MerTK pathway by western blot and corresponding grayscale analysis (compared to the control group) in Raw 264.7 cells after coculture with CT-26 cells exposed to different durations of 254-nm UV.

(C) Transcriptional change in the MerTK pathway in RAW264.7 cells by qPCR analysis.

(D) Western blotting of pro-caspase3/cleaved-caspase 3 expression at different exposure times in the NCM460 cell line and corresponding grayscale analysis (compared to the control group).

(E) Western blotting and grayscale analysis (compared to the control group) of the MerTK pathway in cocultured PBMC-derived macrophages; 0-I: 0 min-stimulation with apoptotic MCM460 + GM-CSF induced PBMCs, which were extracted from patients with inflamed CD; 30-I: 30 min-stimulation with apoptotic NCM460 + GM-CSF induced PBMCs, which were extracted from patients with inflamed CD; 0-F: 0 min-stimulation with apoptotic MCM460 + GM-CSF induced PBMCs, which were extracted from patients with fibrostenotic CD; 30-F: 30 min-stimulation with apoptotic MCM460 + GM-CSF induced PBMCs, which were extracted from patients with fibrostenotic CD; 0-N: 0 min-stimulation with apoptotic MCM460 + GM-CSF induced PBMCs, which were extracted from healthy donors; 30-F: 30 min-stimulation with apoptotic MCM460 + GM-CSF induced PBMCs, which were extracted from healthy donors.

(F) Evaluation of mRNA expression in PBMC-derived macrophages, extracted from patients with CD after coculture with UV-treated NCM460 cells (30 min). All *in vitro* experiments were repeated at least three times to minimize technical and biological variability.

The mechanism by which MerTK recruits ERK for phosphorylation, either directly or through indirect phosphate group transfer to initiate a cascade of amplification reactions, remains elusive. In tumor microenvironment, MerTK autophosphorylation in tumor cells induced phosphorylation of SH2 domain-containing proteins and led to ERK activation. We subsequently performed a nature-IP analysis on gas6-stimulated RAW264.7 to investigate the potential binding between MerTK and ERK (Figure S2A). The findings from the nature-ip experiment did not provide evidence supporting the binding of ERK to MerTK.

Furthermore, GAS6 was employed to stimulate RAW264.7 cells, followed by IP-MS (immunoprecipitation-mass spectrometry) analysis for the identification of proteins that bind with MerTK upon activation. Unfortunately, the peptides of ERK were not found in either untreated or Gas6-treated samples. A total of 600 proteins were identified in Gas6-stimulated samples, excluding the detection of ERK peptides. The IP-MS results indicate that direct activation of MerTK by ERK is not observed, which aligns with previously reported mechanisms (Figure S2B).

MerTK as one of the markers associated with the M2 phenotype has been consistently observed across multiple studies. Next, genes related to macrophage polarization have also undergone changes. We observed increased expression of genes related to classically activated macrophages (M1) [interleukin (IL)-1 β and TNF- α] and alternatively activated macrophages (M2) (IL-10 and arginase-1), after incubation with cells pretreated with UV irradiation. This indicates that a large number of macrophages were polarized during cocubation with apoptotic cells. Longer UV irradiation time (1 or 2 h) led to significantly increased expression of M1-related genes, which was not observed with shorter UV irradiation times (15 and 30 min). This may explain why MerTK phosphorylation decreased with longer irradiation time (Figure 2B) and the transcriptional level gradually decreased (Figure 2C), suggesting that MerTK is not expressed on proinflammatory M1

macrophages. Importantly, a 15-min UV irradiation was sufficient to polarize macrophages to M2 (Figure 2C) and induce the generation of 85% Annexin V⁺ cells,²⁴ corroborating the findings that efferocytosis induces alternatively activated macrophage proliferation.²⁴

Macrophages in normal and pathological intestinal tissues are generated from Ly6C^{hi} monocytes, which originate from bone marrow, enter the peripheral blood circulation, and migrate to the intestine. Self-maintaining macrophages arising from the yolk sac and/or fetal liver are a small part and support enteric neurons or submucosal vasculature in adulthood. Based on this, we extracted peripheral blood mononuclear cells (PBMCs) from patients with CD and stimulated them with GM-CSF. We co-cultured PBMC-derived macrophages and apoptotic NCM460 cells to simulate apoptotic intestinal epithelial cells interacting with macrophages. UV-induced apoptosis was verified by analyzing the levels of caspase3 and cleaved-caspase3 (Figure 2D). We selected a 30-min irradiation to investigate the changes in human cells; at this time, ERK phosphorylation was highest in RAW 264.7 cells (Figure 2B), and cleaved-caspase3 was highest in NCM460 cells (Figure 2D). Similar to the observation in RAW 264.7 cells, apoptotic NCM460 cells activated the MerTK/ERK pathway in macrophages (Figure 2E) and promoted macrophage polarization toward an alternative activated phenotype. This phenotype represents pro-resolving and pro-repair macrophages characterized by increased transcription of arginase-1, IL-10, and TGF- β 1 (Figure 2F). Additionally, we extracted PBMCs from healthy donors and patients with CD plus IF and compared these cells with PBMCs from patients with inflamed CD to determine whether they responded to apoptotic cells differently *in vitro* (Figure 2E). Western blotting did not reveal any significant differences among these three groups, suggesting that the profibrotic profile of macrophages can only be acquired after monocytes enter the gut. The specific intestinal microenvironment in fibrosis progression may remodel the properties and functions of macrophages. Also, we observed reduced levels of phospho-MerTK in the O-F condition (lane 3) compared to O-I (lane 1). This might be attributed to high levels of intestinal and systemic inflammation in active CD.

Our results suggest that apoptotic epithelial cells are capable of activating the MerTK/ERK/TGF- β 1 pathway in intestinal macrophages with growth-promoting, reparative M2 polarization.

MerTK⁺ macrophages activated fibroblasts *in vitro*

To demonstrate the profibrotic activity of MerTK⁺ macrophages, we stimulated MerTK expression in RAW 264.7 cells with Gas6 and evaluated the transcription levels of various profibrotic cytokines, including TGF- β 1, TGF- β 2, TGF- β 3, and platelet-derived growth factor (PDGF). Only TGF- β 1 increased following MerTK activation (Figures 3A and 3B), and 1 h of stimulation with Gas6 resulted in the highest MerTK expression (Figure 3C). After treatment with or without Gas6, we incubated L929 cells with a supernatant of RAW 264.7 cells and performed a wound healing assay to observe the effect of MerTK⁺ macrophage secretions on fibroblast migration (Figures 3D and 3E). The supernatant from Gas6-activated macrophages promoted fibroblast migration, which was most likely due to growth factor secretion.

After knockdown of MerTK (MerTK-KD) in RAW 264.7 cells, the MerTK/ERK pathway was significantly suppressed, and Gas6 could partially rescue this inhibition (Figure 3F). The culture of L929 cells with supernatant from MerTK-KD RAW 264.7 cells showed reduced production of collagen compared with Gas6-stimulated RAW 264.7 and control cells (Figure 3G). The decreased TGF- β 1 production inhibited fibroblast activation and types I and III collagen secretion, which was not reversed by Gas6 (Figure 3G). After MerTK knockdown, Gas6 stimulation did not increase TGF secretion, and as a result, there was no significant increase in collagen secretion from L929 (Figure 3G). These results suggest that the activation of MerTK in macrophages is crucial for collagen production, which is an important cause and pathological manifestation in IF.

Intestinal epithelial cell apoptosis promotes M2 macrophage polarization, activates MerTK on M2 membranes, and induces TGF- β 1 secretion mediated by the ERK1/2 pathway. This results in the activation of fibroblasts and extracellular matrix (ECM) production, which subsequently leads to bowel wall thickening and intestinal obstruction.

OPN upregulated phosphorylation of ERK1/2 in MerTK⁺ macrophages

ERK1/2 is a member of the MAPK family and is activated generically in many inflammatory diseases, including IBD. As a member of the large MAPK family, the biological signals involved in ERK are extremely broad and complex, which also makes ERK unsuitable as a drug target. Knowledge of a possible method that might at least partially control the MerTK/TGF-1 pathway would open up a new possibility for targeted medical treatment of IF.

Based on the co-localization of OPN and MerTK in other fibrotic lesions (as previously described), we investigated the potential connection between MerTK and OPN in the intestine. Western blotting and qPCR revealed an obvious increase in OPN, synchronized with MerTK, in the stenotic intestinal biopsy (Figures 4A and 4B). This synchronous rise was also observed *in vitro*. We treated bone marrow-derived mesenchymal cells and RAW 264.7 cells with Gas6 to activate MerTK; protein expression and transcription of OPN significantly increased (Figures 3A–3D and 4C), as confirmed by its immunofluorescence (Figure 4D). Macrophages, including PBMC-derived macrophages extracted from patients with CD, which were stimulated by apoptotic enterocytes *in vitro*, also showed increased protein expression and transcription of OPN after MerTK activation (Figures 2C–2F). This increasing trend did not diminish with longer UV irradiation times (Figures 2C and 2D), suggesting that apoptosis-activated MerTK⁺ macrophages result in higher OPN production. Immunofluorescence was performed on the same human specimens to assess whether MerTK and OPN exhibited a spatial correlation (Figure 4E). OPN was found to colocalize with MerTK with overlapped fluorescent signals, which were not observed in the control human intestinal mucosa (Figure 4E). OPN knockdown (Figure 4F) restricted the production and secretion of TGF- β 1, instead of TGF- β 2, TGF- β 3, or PDGF (Figure 4G), with no significant change in the protein expression or transcription of MerTK (Figures 4F and 4G). However, MerTK activation by Gas6 after OPN knockdown resulted in a partial recovery of TGF- β 1 production compared to MerTK knockdown (Figure 4G). Although OPN knockdown did not affect

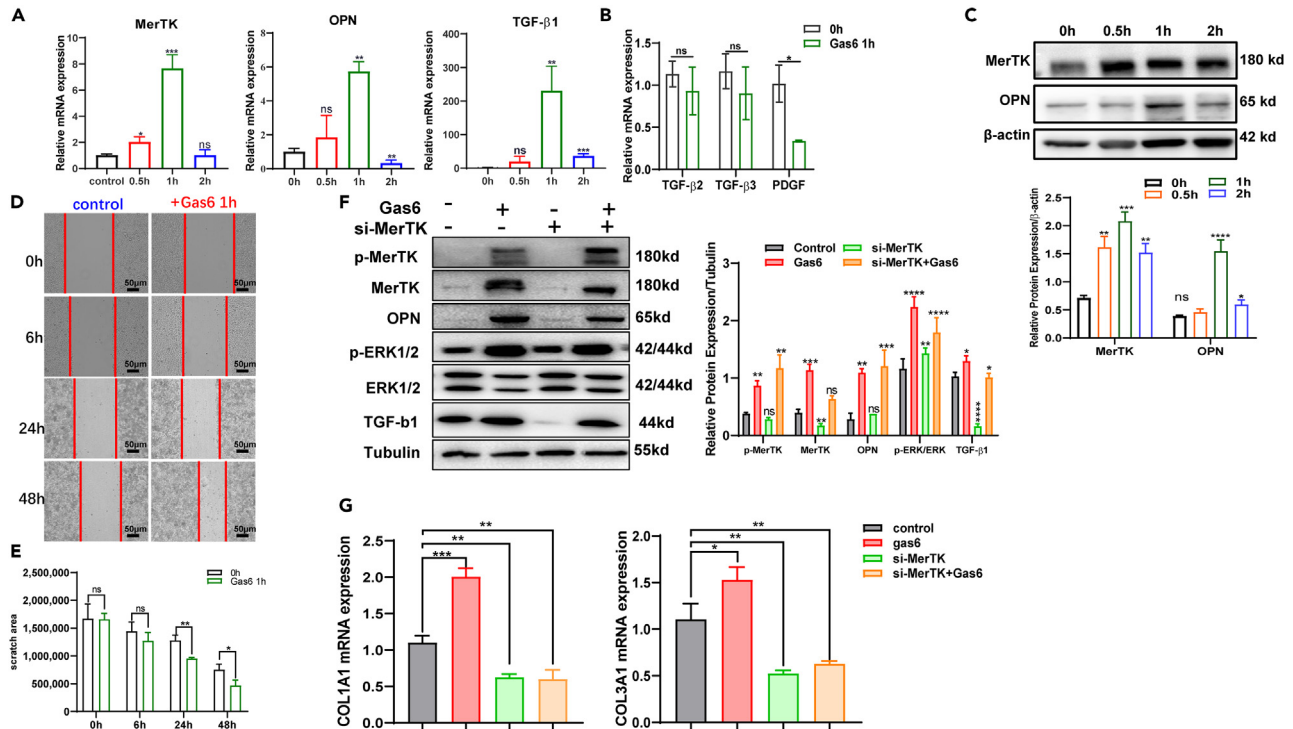


Figure 3. Profibrotic activity of MerTK⁺ macrophages *in vitro*

(A and B) qPCR analysis for MerTK, OPN, TGF- β 1, TGF- β 2, TGF- β 3, and PDGF in RAW264.7 cells after stimulation with 400 ng/mL Gas6. (C) Protein expression evaluation of MerTK and OPN in RAW264.7 cells by western blotting and grayscale analysis (compared to the control group) after stimulation with 400 ng/mL with 0, 30 min, 1 h, and 2 h. (D) Wound healing analysis in L929 cells cultured in the supernatant of RAW 264.7 cells with or without Gas6 stimulation. (E) Quantitative analysis of scratch area in the wound healing experiment by ImageJ. (F) Protein expression evaluation and grayscale analysis (compared to the control group) of MerTK/ERK/TGF pathway after knockdown of MerTK by transfection of siRNA into RAW 264.7 cells with or without Gas6 stimulation; (G) transcriptional evaluation of COL1A1 (left panel) and COL3A1 (right panel) of L929 cells after treatment with the supernatant of RAW264.7 cells. All *in vitro* experiments were repeated at least three times to minimize technical and biological variability.

MerTK expression, it regulated the transcription and exocrine secretion of downstream TGF- β 1, suggesting that OPN can regulate the MerTK signaling pathway without directly influencing MerTK. Next, we explored whether OPN affected TGF- β 1 production by regulating ERK phosphorylation. Phosphorylation of ERK1/2, especially ERK1, was inhibited following OPN knockdown, resulting in decreased production of TGF- β 1 (Figures 4F and 4G). Whether OPN alone increased the production of downstream TGF- β 1 was also evaluated by transfection with plasmids overexpressing OPN. Higher OPN expression alone induced by plasmid transfection, without Gas6 treatment, upregulated ERK1/2 phosphorylation (Figures 4G and 4H), but failed to increase TGF- β 1 production and secretion (Figures 4G and 4I) after a cell supernatant was evaluated by TGF- β 1 ELISA test. These results indicate that OPN can upregulate the MerTK/ERK/TGF- β 1 pathway by affecting ERK1/2 phosphorylation without regulating MerTK.

UNC2025, a MerTK dual inhibitor, alleviated DSS-induced intestinal fibrosis *in vivo*

Considering the important role of the MerTK/TGF pathway in IF development, we administered UNC2025, a potent and orally bioavailable Mer dual inhibitor,³⁰ to DSS-treated C57BL6/J mice, or tap water to the control group (Figure S2C). Consistent with our findings in human specimens, increased apoptosis was identified in the murine colon with a strengthened fluorescence signal of cleaved-caspase 3 (Figure S2D). In the experimental DSS- and TNBS-induced IF, both MerTK and OPN exhibited higher transcription and protein expression levels (Figures 5A, 5B, and S4A). In addition, MerTK was found to colocalize with CD206 and OPN (Figure S2E). In DSS-induced fibrosis, increased TGF- β 1 transcription levels were observed with changes in MerTK and OPN (Figures 5B and S3A). The alteration in Gas6 transcription appeared subtle but was still substantial (Figure 5B). We examined MerTK expression in the experimental colitis group to determine whether it had a similar change as seen in the human samples. The results showed similarity, with less obvious changes in OPN (Figure 5A). Immunohistochemical staining for MerTK verified this alteration (Figure S3B). Based on the change in MerTK expression, we focused on the effects of oral UNC2025 in experimental mice. Masson's trichrome staining revealed increased deposition of collagen in mice treated with 2% dextran sodium salt (DSS) for 64 days, and light microscopy demonstrated a thicker intestinal wall and narrower lumen (Figures 5C and S4B). More

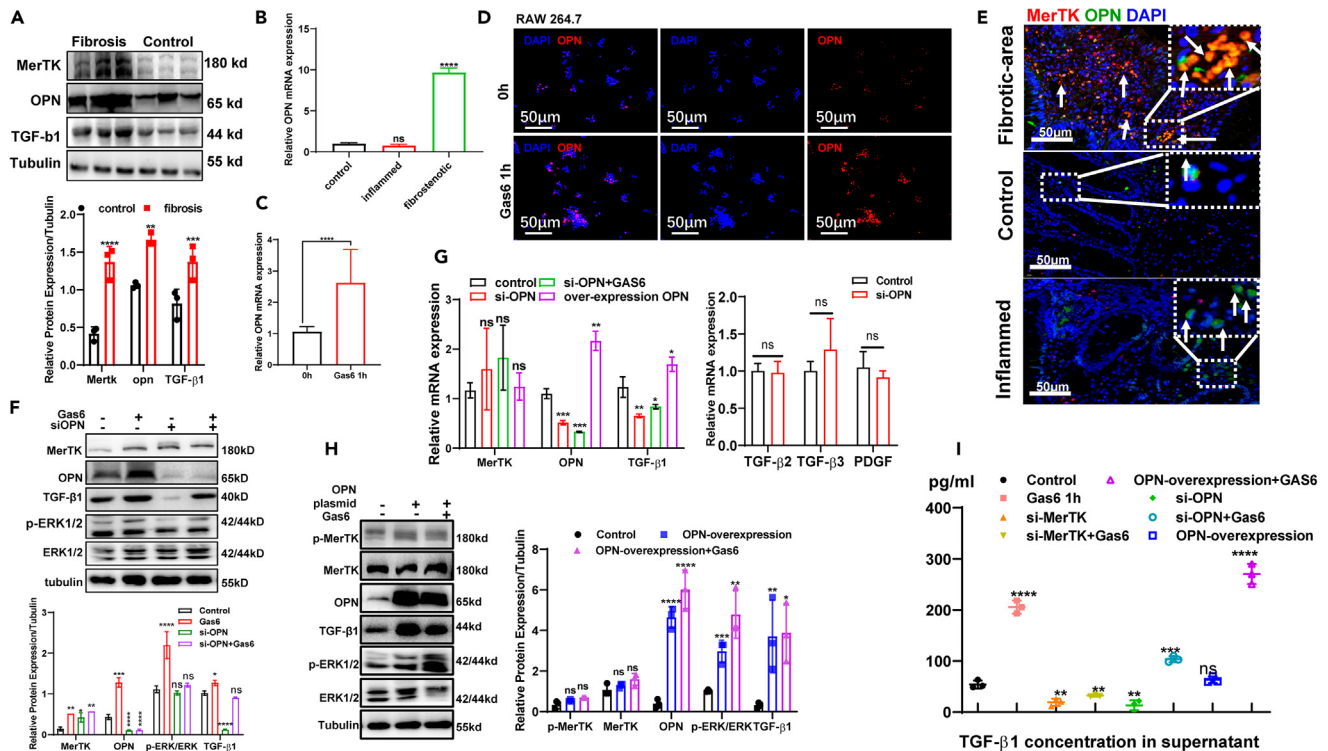


Figure 4. OPN regulated TGF-β1 secretion induced by MerTK activation

(A and B) Evaluation of MerTK and OPN by western blotting, grayscale analysis (compared to the control group), and qPCR in intestinal specimens from patients with CD.

(C) Transcriptional level of OPN in RAW 264.7 cells after 1 h of 400 ng/mL Gas6 stimulation.

(D) Intracellular signal intensity of OPN in RAW 264.7 cells with or without 1-h Gas6 stimulation for immunofluorescence analysis.

(E) Immunofluorescence staining and colocalization of MerTK and OPN in human specimens.

(F) Changes in the MerTK pathway after knockdown of OPN with siRNA for western blotting and corresponding grayscale analysis (compared to the control group).

(G) Transcriptional change (compared to the control group) in the MerTK pathway and TGF-β2, TGF-β3, and PDGF after knockdown of OPN or overexpression with plasmid transfection for qPCR analysis (control: vector transfected; siOPN: small interfering OPN RNA transfected).

(H) Changes in the MerTK pathway after OPN overexpression with plasmid transfection for western blotting and grayscale analysis (compared to the control group).

(I) TGF-β1 ELISA test for supernatants of RAW 264.7 cells (compared to the control group). All *in vitro* experiments were repeated at least three times to minimize technical and biological variability.

deposition of types I and III collagen confirmed the fibrotic pathological change after 64 days of DSS treatment, as evaluated by qPCR, western blotting, and immunohistochemistry (Figures 5B, 5D, and S3C). These results suggested that the change in MerTK was in step with the deposition of ECM, mainly collagen. Despite their important and non-negligible roles in mediating wound healing during the initial phase of inflammation, MerTK⁺ macrophages may undergo excessive repair as inflammation progresses.

Considering that most patients with CD plus IF present advanced or progressive stages of the disease when they seek medical treatment, we administered UNC2025 to mice at different stages (Day 0/Day 21/Day 42) to mimic the clinical treatment of early, middle, and late fibrosis. Masson's trichrome staining and immunohistochemistry of collagen showed that oral UNC2025 (3 mg/kg) reduced ECM deposition and alleviated fibrosis (Figures 5C, S3C, and S4B). Relative quantification of COL1A1, COL3A1, and COL4A1 by qPCR demonstrated the therapeutic effect of UNC2025 (Figure 5B). Western blotting supported the decrease in MerTK expression after UNC2025 treatment (Figure 5D), demonstrating that this small molecule MerTK inhibitor, UNC2025, exhibits great biological activity and targeted inhibition *in vivo*. We also noted that the antifibrotic effect of the inhibitor UNC2025 gradually decreased as the administration duration was prolonged (Figures 5B–5D and S3C). Immunohistochemical staining confirmed reduced MerTK expression in the mouse colon (Figure S3B). Shortening of the drug course also reduced the inhibitory effect of UNC2025 on MerTK expression (Figure 5D). The change in immunohistochemical staining was not as obvious as that observed in human intestinal tissue. This may be attributed to nonspecific immunohistochemical staining, and the DSS-induced experimental model may be ineffective in reproducing the intestinal microenvironment in human CD. Light microscopy revealed change in the intestinal wall and lumen compared to that in 64-day DSS-treated mice without UNC2025 treatment (Figure 5C). With the change in MerTK expression, OPN transcription and protein expression levels tended to decrease, and TGF-β1 showed a synchronous

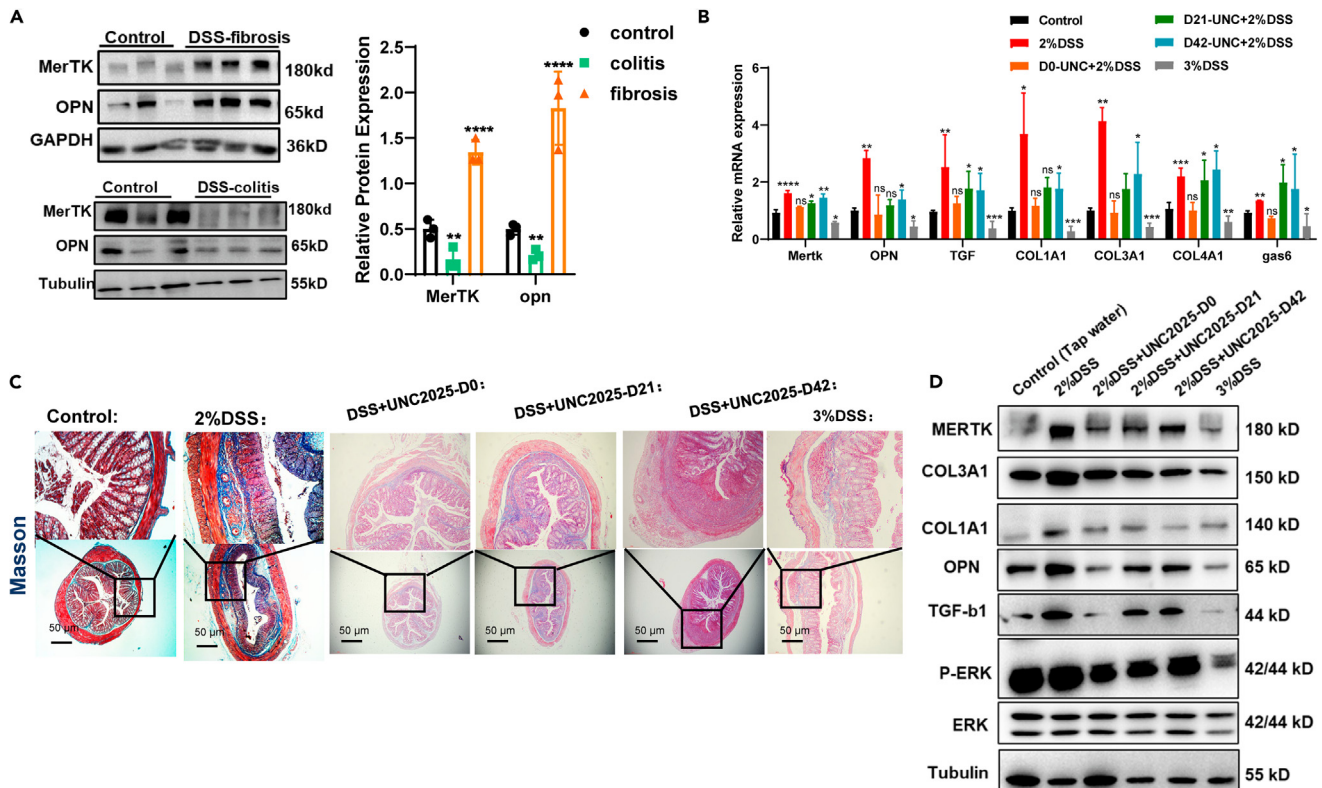


Figure 5. UNC225, an inhibitor of MerTK, alleviated DSS-induced intestinal fibrosis

(A) Western blot and grayscale analysis of MerTK and OPN in experimental mice with acute colitis or chronic fibrosis ($n = 3$).

(B) qPCR evaluation of MerTK, OPN, Gas6, TGF- β 1, COL1A1, and COL3A1 in mice ($n = 3$).

(C) Masson's trichrome staining of the colon in mice ($n = 3$).

(D) Protein evaluation by western blotting of the MerTK pathway and OPN in different groups and corresponding grayscale analysis (Control: mice treated with tap water; DSS: 64-day 2% DSS-treated mice; DSS + UNC225-D0: mice treated with 3 mg/kg UNC225 from the first day; 2% DSS + UNC225-D21: mice treated with 3 mg/kg UNC225 from day 21; 2% DSS + UNC225-D42: mice treated with 3 mg/kg UNC225 from day 42; $n = 3$).

change (Figure 5D). The MerTK/ERK/TGF pathway was also inhibited following UNC225 treatment (Figure 5D). The inhibitory effect was markedly reduced as the drug course was shortened. These results suggested that IF and TGF- β 1 secretions were inhibited when MerTK activation was blocked. Notably, targeting MerTK shows therapeutic promise in mice. Medication administered early in the progression of an illness is essential for therapeutic effectiveness and long-term outcomes.

Maintaining the delicate balance between pro-inflammatory and anti-inflammatory responses is a key aspect of tissue homeostasis. We observed an aberrant decrease in MerTK expression both in acute colitis model mice (3%DSS) and intestinal specimens from active CD patients. As a crucial anti-inflammatory signal, proper functioning of MerTK signaling is indispensable for inflammation resolution. The abnormal reduction in MerTK signaling may significantly contribute to exacerbation of inflammation in CD.

Therefore, precise regulation of MerTK signaling is of paramount importance throughout the chronic progression of CD. To assess the impact of the MerTK inhibitor, UNC225, on disease severity, we evaluated mouse body weight and colon length at the conclusion of the 64-day model establishment period (Figure S4C). No significant differences in body weight or colon length were observed among the experimental groups. The sacrificed mice did not exhibit any signs of bloody stools or loose stools. This could be attributed to the lower concentration of DSS used for chronic enteritis induction and an extended recovery period for enteritis development.

Our results demonstrated that OPN regulated the MerTK/ERK/TGF pathway in intestinal macrophages, and UNC225, especially when administered early, could relieve IF in a mouse model of DSS-induced chronic colitis (Figure 6). Overall, IF now has a promising potential therapeutic target.

DISCUSSION

Here, we first revealed a possible link between MerTK, an important member of the TAM family, and the complex fibrotic course of CD. The primary finding of this study is the identification of a molecular mechanism of IF in CD mediated by the MerTK/ERK/TGF- β 1 pathway. OPN regulates ERK1/2 activation, which in turn affects downstream TGF- β 1 secretion, thereby increasing fibroblast activation, ECM deposition,

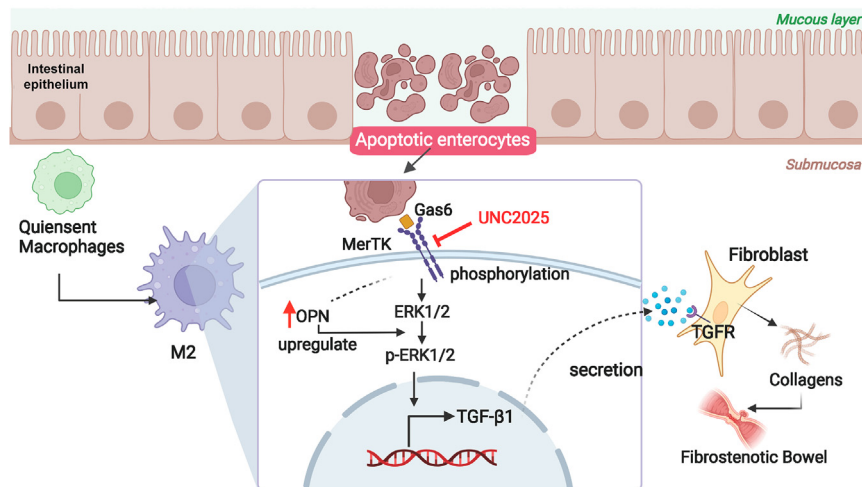


Figure 6. A schematic model: MerTK⁺ macrophages mediated intestinal fibrosis in CD

Apoptotic epithelial cells activated MerTK on intestinal macrophages and promoted monocytes polarized to an alternatively activated type. Phosphorylated MerTK on the membrane increased OPN and induced ERK1/2 activation, leading to more TGF- β 1 production and secretion. Increased OPN upregulated ERK1/2 phosphorylation, resulting in increased TGF transcription. Secreted TGF- β 1 activated fibroblasts, resulting in increased collagen deposition. Targeting MerTK with UNC2025 alleviated intestinal fibrosis *in vivo*.

and IF (Figure 6). We provided correlative evidence for this pathway in humans, DSS-treated mice, and *in vitro* experiments. The MerTK expression level was lower in the active inflamed bowel in patients with CD but significantly increased during the progression to IF accompanied by continuous penetrating intestinal inflammation. Our animal and cell experiments confirmed these findings. In addition, we attempted to determine what activated the MerTK pathway and how it contributed to IF development. Apoptotic enterocytes, efferocytosis activators, may be the main factor that promotes increased MerTK expression. This increased MerTK phosphorylation induced ERK activation and resulted in increased TGF- β 1 secretion. The MerTK/ERK pathway has been found in other diseases, including cancer and nonalcoholic steatohepatitis.¹⁷ To elucidate the involvement of macrophage MerTK signaling in fibrogenesis, exogenous Gas6 was employed to activate macrophage MerTK signaling in this study. Activation of MerTK signaling in macrophages stimulates fibroblasts through exocrine TGF- β 1 secretion. The content presented herein serves as one piece of evidence supporting the notion that MerTK⁺ macrophages exert their profibrotic function.

The Gas6/MerTK signaling pathway has been extensively investigated in the field of tumor and immunity, while this study represents the first discussion of its involvement in fibrotic IBD. We believe that our study is the first to reveal the partial function of this pathway in CD and related complications. A recent study demonstrated that AXL, another member of the TAM family, may have a profibrotic function by activating fibroblasts in fibrosis development.³¹ Therefore, the direct influence of residual Gas6 in the supernatant on fibroblast activation in the wound healing assay cannot be ruled out. This was one of the limitations of this study. However, in the qPCR analysis of RAW 264.7 and L929 coculture experiments, MerTK knockdown in RAW 264.7 cells reduced L929 cell activation, which was not reversed by Gas6 stimulation. This indicates the profibrotic activity of MerTK⁺ macrophages, but the interaction effect between residual Gas6 and AXL on fibroblasts was insignificant.

Soluble Mer released in peripheral blood has been linked to disease activity in several autoimmune diseases,³² where it results in decreased activation of MerTK and downstream pathways. A higher level of ADAM17 activity detected in actively inflamed intestines may explain the lower level of MerTK intestinal expression in patients with active CD. Additionally, current research primarily suggests that MerTK is indicative of anti-inflammatory/pro-repair macrophage differentiation. Therefore, the diminished expression of MerTK in macrophages may also contribute to the progression of inflammation in individuals with CD. We cannot reach a conclusive judgment based on the available facts; thus, additional research on inflammation is necessary. After ERK1/2 phosphorylation, additional transcription is induced via p-ERK1/2 activation of the TGF transcription factor activator protein-1 to increase TGF production.³³ TGF- β is one of the most important profibrotic factors in fibrotic diseases, including IF. Clinical or preclinical medicine targeting TGF- β is available, such as pirfenidone, although it has not been approved for use in IF. In addition, TGF- β is reported to increase in the affected mucosa in patients with active UC or CD and is correlated with disease duration.³⁴ In this study, we did not find any obvious increase in inflamed areas. This may have been due to heterogeneity in patients based on different disease durations.

Intestinal quiescent macrophages are predominantly polarized into two well-established polarized phenotypes, classically (M1) and alternatively activated (M2) macrophages, after receiving endogenous and exogenous stimuli. M2-biased polarization is rapidly initiated and often observed under inflammation. However, MerTK expression did not appear to be fully synchronized with it, as we observed in human inflamed samples. Cai *B et al.* found that neither loss nor cleavage resistance of MerTK in mice would affect total macrophage density and polarization.³⁵ However, MerTK-mediated efferocytosis, which is mainly initiated by apoptotic cells, has been found to be a critical driving force for

M2-macrophage polarization and maintenance.^{14,23} This corroborates our findings of apoptotic intestinal epithelium-induced activation of MerTK/ERK signaling in intestinal macrophages. This also indicates that MerTK⁺ macrophages are more likely to play a role in promoting repair and fibrosis and that the mere presence of M2 cells might not be the main threat to fibrosis. Notably, apoptosis also occurred in the intestinal mucosa in areas of inflammation, but MerTK signaling was inhibited, suggesting that the MerTK-inhibiting factors during the inflammatory phase are significantly more active. The previously described increased activity of ADAM17 in actively inflamed intestines may explain this phenomenon.³⁶ MerTK cleavage is performed by endogenous ADAM17 protease,³⁷ which limits MerTK expression and activity in macrophages. Given the reported anti-inflammatory role of MerTK, decreased expression of MerTK in active CD and acute murine colitis may be associated with high levels of inflammatory activity.

Maintaining the delicate balance between pro-inflammatory and anti-inflammatory responses is a key aspect of tissue homeostasis. We observed an aberrant decrease in MerTK expression both in acute colitis model mice (3%DSS) and intestinal specimens from active CD patients. As a crucial anti-inflammatory signal, proper functioning of MerTK signaling is indispensable for inflammation resolution. The abnormal reduction in MerTK signaling may significantly contribute to exacerbation of inflammation in CD. Therefore, precise regulation of MerTK signaling holds paramount importance throughout the chronic progression of CD. While moderate activation of MerTK signaling proves beneficial during inflammation resolution, sustained activation becomes a pivotal driver of fibrosis during the reparative phase following inflammation resolution. Further studies are needed to explore the exact mechanisms by which intestinal inflammation suppresses the function of MerTK⁺ macrophages.

In addition, we have identified for the first time that intracellular OPN can enhance the activation of MerTK signaling pathway and contribute to the development of IF. Based on recent reports of the potential connection between OPN and MerTK in some fibrotic tissues, such as single-cell sequence analysis in IPF²⁷ and tissue repair after myocardial infarction,²⁵ we supposed that OPN may have some effect on MerTK. We conducted a series of knockdown experiments to investigate the possible association: OPN upregulated ERK1/2 phosphorylation, mainly affecting ERK1 without affecting MerTK, and ultimately increased TGF- β 1 secretion, resulting in fibrosis. There are exocrine and intracellular (iOPN) forms of OPN. We did not explore which form participated in this regulatory function, and studies on iOPN are insufficient to determine its specific biological functions and molecular mechanisms. Further research on iOPN is thus needed. However, we suspect that the intracellular OPN regulates the MerTK/TGF pathway, considering the intracellular location of ERK. Meanwhile, which form of OPN plays a profibrotic role in IF requires investigation. In this study, we found that MerTK activation resulted in increased OPN expression in macrophages, with no feedback upregulation when OPN was overexpressed.

We demonstrated that blocking MerTK signaling with UNC2025 abolished fibrogenic gene and protein expression in response to apoptotic cells and cytokines under chronic inflammation. The decreased deposition of collagen is the best illustration, and changes in intestinal wall thickness observed under light microscopy also proved its curative effect. UNC2025 is a small molecule-targeted inhibitor that does not inhibit AXL. The antifibrotic efficacy of UNC2025 in this study was independent of the AXL pathway. We found that early inhibition of the MerTK pathway by UNC2025 showed a better antifibrotic effect than later intervention, probably because MerTK signaling in intestinal macrophages mainly induces collagen fiber production but does not affect the fibrin degradation process. During long-term fibrogenesis progression, a combination of drugs that inhibit collagen production and promote collagen degradation is the most desirable choice.

This study provides a promising direction for the medical therapy of IF in CD. Although nintedanib and pirfenidone have been approved as antifibrotics in pulmonary fibrosis, no antifibrotic drugs exist for use in the intestines or any organ other than the lungs. At present, the main thrust of drug therapy for IF is still anti-inflammatory medication, and anti-TNF antibodies are currently the most effective drugs available in specific cases of stricturing CD since the advent of biologics. However, even in combination therapy (immunosuppressant or adalimumab), intestinal resection remains unavoidable, with the median surgery time being 3.8 years, according to the results of a French multicenter, prospective, observational cohort (CREOLE) study.³⁸ To avoid intestinal resection or even endoscopic dilation, medical therapy, especially a specific intestinal antifibrotic agent, remains a major challenge. Drug therapy targeting the TAM family has made much progress in recent years, mainly in the field of tumor monoclonal antibody therapy or in resolving inflammation. Because MerTK plays an immunosuppressive role in the immune response, inhibiting or blocking it by UNC2025 may cause more severe bowel inflammation, especially if the drug is taken during the active phase of the disease. The DSS model utilized in this study was 2% less concentrated than the acute colitis model, which may have been one of the reasons why we did not notice evident inflammation over the 64-day modeling period. Except for intestinal wall thickening and ECM deposition, H&E staining revealed no obvious difference between immune cell infiltration and intestinal mucosal integrity. A more accurate evaluation of the inflammation level is necessary, which was one of the limitations of this study. Because we must carefully maintain a delicate balance between healing and fibrosis, arbitrarily blocking all healing mechanisms is inappropriate. In the meantime, focusing only on inflammatory mechanisms is completely inadequate for fibrosis treatment. However, targeting the TAM family appears to be a good choice, given its paradoxical function in inflammation and fibrosis. Combination with anti-inflammatory therapy should be considered in different phases of the disease. In addition, while employing the inhibitor in clinical practice, careful consideration should be given to both the dosage and duration of administration. The use of 3 mg/kg UNC2025 in this study was based on previously published *in vivo* research,³⁰ which showed the inhibition of MerTK phosphorylation and downstream pathways.

In this context, we reported our observation of the dynamic changes in MerTK expression during CD development. MerTK is decreased in the active inflammatory bowel and increased in the stenotic bowel. We showed that apoptotic enterocytes activated the MerTK-ERK1/2-TGF- β 1 pathway in macrophages, promoting IF development. MerTK activation resulted in increased OPN expression in macrophages. OPN upregulated ERK1/2 phosphorylation, which in turn affected TGF- β 1 secretion, but no feedback effect on MerTK from OPN was

observed. Increased TGF- β secretion further activated fibroblasts, leading to more ECM deposition. UNC2025, an orally bioavailable MerTK dual inhibitor, alleviated IF induced by chronic colitis in DSS-treated mice. These findings provide a potential target, MerTK, for IF treatment in CD.

Limitations of the study

The number of available human samples was insufficient in our work, and the heterogeneity of the patients is a limitation. Whether other downstream pathways of MerTK also influence fibrosis needs to be analyzed in future studies. We also hope to remedy related limitations in the following work and further characterize the relationship between acute inflammation and MerTK. In the *in vitro* experiments investigating the interaction between fibroblasts and macrophages, we used L929 cell line as a substitute for primary fibroblasts. Prolonged passaging of cells inevitably leads to genomic alterations within the cell line, which will not adequately mimic the disease state. The indispensability of primary cells represents one of the current limitations inherent in this study. We anticipate that future investigations will explore the anti-fibrotic efficacy of targeted inhibition of MerTK using a larger cohort encompassing patient samples.

STAR★METHODS

Detailed methods are provided in the online version of this paper and include the following:

- KEY RESOURCES TABLE
- RESOURCE AVAILABILITY
 - Lead contact
 - Materials availability
 - Data and code availability
- EXPERIMENTAL MODEL AND STUDY PARTICIPANT DETAILS
 - Ethical approval for human and animal studies
 - Human sample collection and analysis
 - Mice
 - Experimental models of chronic colitis
- METHOD DETAILS
 - Histology, immunohistochemistry, and immunofluorescence
 - Cell culture and transfection
 - Generation of apoptotic cells
 - ELISA
 - Quantitative real-time PCR
 - Western blotting
 - Wound healing assay
 - LC-MS analysis
- QUANTIFICATION AND STATISTICAL ANALYSIS

SUPPLEMENTAL INFORMATION

Supplemental information can be found online at <https://doi.org/10.1016/j.isci.2024.110226>.

ACKNOWLEDGMENTS

Figure 6 was completed by BioRender, and we thank Yifan Bao for helping us polish the figures. We have been authorized to use Figure 6 and have received the publishing license. This work was financially supported by National Natural Science Foundation of China (82072223).

AUTHOR CONTRIBUTIONS

Conceptualization, J.L. and J.R.; methodology, P.L., C.W., and W.G.; investigation, H.J. and C.W.; writing – original draft, J.L. and Y.L.; writing – review and editing, J.L., X.W., Y.Z., and J.R.; funding acquisition, J.R.; resources, X.W. and Y.Z.; supervision, J.R.

DECLARATION OF INTERESTS

Authors do not have any possible conflicts of interest.

Received: November 8, 2023

Revised: April 4, 2024

Accepted: June 6, 2024

Published: June 8, 2024

REFERENCES

- Ng, W.K., Wong, S.H., and Ng, S.C. (2016). Changing epidemiological trends of inflammatory bowel disease in Asia. *Intest. Res.* 14, 111–119. <https://doi.org/10.5217/ir.2016.14.2.111>.
- Lawrance, I.C., Rogler, G., Bamias, G., Breynaert, C., Florholmen, J., Pellino, G., Reif, S., Specia, S., and Latella, G. (2017). Cellular and Molecular Mediators of Intestinal Fibrosis. *J. Crohns Colitis* 11, 1491–1503. <https://doi.org/10.1016/j.crohns.2014.09.008>.
- Yamamoto, T., Fazio, V.W., and Tekkis, P.P. (2007). Safety and efficacy of stricturoplasty for Crohn's disease: a systematic review and meta-analysis. *Dis. Colon Rectum* 50, 1968–1986. <https://doi.org/10.1007/s10350-007-0279-5>.
- Wu, F., and Chakravarti, S. (2007). Differential expression of inflammatory and fibrogenic genes and their regulation by NF-kappaB inhibition in a mouse model of chronic colitis. *J. Immunol.* 179, 6988–7000. <https://doi.org/10.4049/jimmunol.179.10.6988>.
- di Mola, F.F., Friess, H., Scheuren, A., Di Sebastiano, P., Graber, H., Egger, B., Zimmermann, A., Korc, M., and Büchler, M.W. (1999). Transforming growth factor-betas and their signaling receptors are coexpressed in Crohn's disease. *Ann. Surg.* 229, 67–75. <https://doi.org/10.1097/00000658-199901000-00009>.
- Tang, P.M.K., Nikolai-Paterson, D.J., and Lan, H.Y. (2019). Macrophages: versatile players in renal inflammation and fibrosis. *Nat. Rev. Nephrol.* 15, 144–158. <https://doi.org/10.1038/s41581-019-0110-2>.
- Aehnlich, P., Powell, R.M., Peeters, M.J.W., Rahbech, A., and Thor Straten, P. (2021). TAM Receptor Inhibition-Implications for Cancer and the Immune System. *Cancers* 13, 1195. <https://doi.org/10.3390/cancers13061195>.
- Smirne, C., Rigamonti, C., De Benedittis, C., Sainaghi, P.P., Bellan, M., Burlone, M.E., Castello, L.M., and Avanzi, G.C. (2019). Gas6/TAM Signaling Components as Novel Biomarkers of Liver Fibrosis. *Dis. Markers* 2019, 2304931. <https://doi.org/10.1155/2019/2304931>.
- Nicolas-Avila, J.A., Lechuga-Vieco, A.V., Esteban-Martinez, L., Sanchez-Diaz, M., Diaz-Garcia, E., Santiago, D.J., Rubio-Ponce, A., Li, J.L., Balachander, A., Quintana, J.A., et al. (2020). A Network of Macrophages Supports Mitochondrial Homeostasis in the Heart. *Cell* 183, 94–109.e23. <https://doi.org/10.1016/j.cell.2020.08.031>.
- Gordon, I.O., Agrawal, N., Goldblum, J.R., Fiocchi, C., and Rieder, F. (2014). Fibrosis in ulcerative colitis: mechanisms, features, and consequences of a neglected problem. *Inflamm. Bowel Dis.* 20, 2198–2206. <https://doi.org/10.1097/mib.0000000000000080>.
- Wu, H., Zheng, J., Xu, S., Fang, Y., Wu, Y., Zeng, J., Shao, A., Shi, L., Lu, J., Mei, S., et al. (2021). Mer regulates microglial/macrophage M1/M2 polarization and alleviates neuroinflammation following traumatic brain injury. *J. Neuroinflammation* 18, 2. <https://doi.org/10.1186/s12974-020-02041-7>.
- Triantafyllou, E., Pop, O.T., Possamai, L.A., Wilhelm, A., Liaskou, E., Singanayagam, A., Bernsmeier, C., Kamri, W., Petts, G., Dargue, R., et al. (2018). MerTK expressing hepatic macrophages promote the resolution of inflammation in acute liver failure. *Gut* 67, 333–347. <https://doi.org/10.1136/gutjnl-2016-313615>.
- Du, W., Zhu, J., Zeng, Y., Liu, T., Zhang, Y., Cai, T., Fu, Y., Zhang, W., Zhang, R., Liu, Z., and Huang, J.A. (2021). KPNB1-mediated nuclear translocation of PD-L1 promotes non-small cell lung cancer cell proliferation via the Gas6/MerTK signaling pathway. *Cell Death Differ.* 28, 1284–1300. <https://doi.org/10.1038/s41418-020-00651-5>.
- DeBerge, M., Yeap, X.Y., Dehn, S., Zhang, S., Grigoryeva, L., Misener, S., Prociassi, D., Zhou, X., Lee, D.C., Muller, W.A., et al. (2017). MerTK Cleavage on Resident Cardiac Macrophages Compromises Repair After Myocardial Ischemia Reperfusion Injury. *Circ. Res.* 121, 930–940. <https://doi.org/10.1161/CIRCRESAHA.117.31327>.
- Zhen, Y., Finkelman, F.D., and Shao, W.H. (2018). Mechanism of Mer receptor tyrosine kinase inhibition of glomerular endothelial cell inflammation. *J. Leukoc. Biol.* 103, 709–717. <https://doi.org/10.1002/JLB.3A0917-368R>.
- Bellan, M., Cittone, M.G., Tonello, S., Rigamonti, C., Castello, L.M., Gavelli, F., Pirisi, M., and Sainaghi, P.P. (2019). Gas6/TAM System: A Key Modulator of the Interplay between Inflammation and Fibrosis. *Int. J. Mol. Sci.* 20, 5070.
- Cai, B., Dongiovanni, P., Corey, K.E., Wang, X., Shmarakov, I.O., Zheng, Z., Kasikara, C., Davra, V., Meroni, M., Chung, R.T., et al. (2020). Macrophage MerTK Promotes Liver Fibrosis in Nonalcoholic Steatohepatitis. *Cell Metab.* 31, 406–421.e7. <https://doi.org/10.1016/j.cmet.2019.11.013>.
- Rovati, L., Kaneko, N., Pedica, F., Monno, A., Maehara, T., Perugino, C., Lanzillotta, M., Pecetta, S., Stone, J.H., Doglioni, C., et al. (2021). Mer tyrosine kinase as a possible link between resolution of inflammation and tissue fibrosis in IgG4-related disease. *Rheumatology* 60, 4929–4941. <https://doi.org/10.1093/rheumatology/keab096>.
- Lemke, G. (2019). How macrophages deal with death. *Nat. Rev. Immunol.* 19, 539–549. <https://doi.org/10.1038/s41577-019-0167-y>.
- Brynskov, J., Foegh, P., Pedersen, G., Ellervik, C., Kirkegaard, T., Bingham, A., and Saermark, T. (2002). Tumour necrosis factor alpha converting enzyme (TACE) activity in the colonic mucosa of patients with inflammatory bowel disease. *Gut* 51, 37–43.
- Blaydon, D.C., Biancheri, P., Di, W.-L., Plagnol, V., Cabral, R.M., Brooke, M.A., van Heel, D.A., Ruschendorf, F., Toynbee, M., Walne, A., et al. (2011). Inflammatory Skin and Bowel Disease Linked to ADAM17 Deletion. *N. Engl. J. Med.* 365, 1502–1508. <https://doi.org/10.1056/NEJMoa1100721>.
- Moss, M.L., and Minond, D. (2017). Recent Advances in ADAM17 Research: A Promising Target for Cancer and Inflammation. *Mediators Inflamm.* 2017, 9673537. <https://doi.org/10.1155/2017/9673537>.
- Stanford, J.C., Young, C., Hicks, D., Owens, P., Williams, A., Vaught, D.B., Morrison, M.M., Lim, J., Williams, M., Brantley-Sieders, D.M., et al. (2014). Efferocytosis produces a prometastatic landscape during postpartum mammary gland involution. *J. Clin. Invest.* 124, 4737–4752. <https://doi.org/10.1172/jci76375>.
- Gerlach, B.D., Ampomah, P.B., Yurdagül, A., Jr., Liu, C., Lauring, M.C., Wang, X., Kasikara, C., Kong, N., Shi, J., Tao, W., and Tabas, I. (2021). Efferocytosis induces macrophage proliferation to help resolve tissue injury. *Cell Metab.* 33, 2445–2463.e8. <https://doi.org/10.1016/j.cmet.2021.10.015>.
- Shirakawa, K., Endo, J., Kataoka, M., Katsumata, Y., Anzai, A., Moriyama, H., Kitakata, H., Hiraide, T., Ko, S., Goto, S., et al. (2020). MerTK Expression and ERK Activation Are Essential for the Functional Maturation of Osteopontin-Producing Reparative Macrophages After Myocardial Infarction. *J. Am. Heart Assoc.* 9, e017071. <https://doi.org/10.1161/jaha.120.017071>.
- Shen, X., Qiu, Y., Wight, A.E., Kim, H.J., and Cantor, H. (2022). Definition of a mouse microglial subset that regulates neuronal development and proinflammatory responses in the brain. *Proc. Natl. Acad. Sci. USA* 119, e2116241119. <https://doi.org/10.1073/pnas.2116241119>.
- Morse, C., Tabib, T., Sembrat, J., Buschur, K.L., Bittar, H.T., Valenzi, E., Jiang, Y., Kass, D.J., Gibson, K., Chen, W., et al. (2019). Proliferating SPP1/MERTK-expressing macrophages in idiopathic pulmonary fibrosis. *Eur. Respir. J.* 54, 1802441. <https://doi.org/10.1183/13993003.02441-2018>.
- Hunter, C., Bond, J., Kuo, P.C., Selim, M.A., and Levinson, H. (2012). The role of osteopontin and osteopontin aptamer (OPN-R3) in fibroblast activity. *J. Surg. Res.* 176, 348–358. <https://doi.org/10.1016/j.jss.2011.07.054>.
- Shelley-Fraser, G., Borley, N.R., Warren, B.F., and Shepherd, N.A. (2012). The connective tissue changes of Crohn's disease. *Histopathology* 60, 1034–1044. <https://doi.org/10.1111/j.1365-2559.2011.03911.x>.
- Zhang, W., DeRyckere, D., Hunter, D., Liu, J., Stashko, M.A., Minson, K.A., Cummings, C.T., Lee, M., Glaros, T.G., Newton, D.L., et al. (2014). UNC2025, a potent and orally bioavailable MER/FLT3 dual inhibitor. *J. Med. Chem.* 57, 7031–7041. <https://doi.org/10.1021/jm500749d>.
- Steiner, C.A., Rodansky, E.S., Johnson, L.A., Berinstein, J.A., Cushing, K.C., Huang, S., Spence, J.R., and Higgins, P.D.R. (2021). AXL Is a Potential Target for the Treatment of Intestinal Fibrosis. *Inflamm. Bowel Dis.* 27, 303–316. <https://doi.org/10.1093/ibd/izaa169>.
- Zizzo, G., Guerrieri, J., Dittman, L.M., Merrill, J.T., and Cohen, P.L. (2013). Circulating levels of soluble MER in lupus reflect M2c activation of monocytes/macrophages, autoantibody specificities and disease activity. *Arthritis Res. Ther.* 15, R212. <https://doi.org/10.1186/ar4407>.
- Liu, G., Ding, W., Liu, X., and Mulder, K.M. (2006). c-Fos is required for TGFbeta1 production and the associated paracrine migratory effects of human colon carcinoma cells. *Mol. Carcinog.* 45, 582–593. <https://doi.org/10.1002/mc.20189>.
- Babyatsky, M.W., Rossiter, G., and Podolsky, D.K. (1996). Expression of transforming growth factors alpha and beta in colonic mucosa in inflammatory bowel disease. *Gastroenterology* 110, 975–984. <https://doi.org/10.1053/gast.1996.v110.pm8613031>.
- Cai, B., Thorp, E.B., Doran, A.C., Subramanian, M., Sansbury, B.E., Lin, C.S., Spite, M., Fredman, G., and Tabas, I. (2016). MerTK cleavage limits proresolving mediator

- biosynthesis and exacerbates tissue inflammation. *Proc. Natl. Acad. Sci. USA* 113, 6526–6531. <https://doi.org/10.1073/pnas.1524292113>.
36. Cesaro, A., Abakar-Mahamat, A., Brest, P., Lassalle, S., Selva, E., Filippi, J., Hébuterne, X., Hugot, J.-P., Doglio, A., Galland, F., et al. (2009). Differential expression and regulation of ADAM17 and TIMP3 in acute inflamed intestinal epithelia. *Am. J. Physiol. Gastrointest. Liver Physiol.* 296, G1332–G1343. <https://doi.org/10.1152/ajpgi.90641.2008>.
37. Thorp, E., Vaisar, T., Subramanian, M., Mautner, L., Blobel, C., and Tabas, I. (2011). Shedding of the Mer tyrosine kinase receptor is mediated by ADAM17 protein through a pathway involving reactive oxygen species, protein kinase C δ , and p38 mitogen-activated protein kinase (MAPK). *J. Biol. Chem.* 286, 33335–33344. <https://doi.org/10.1074/jbc.M111.263020>.
38. Bouhnik, Y., Carbonnel, F., Laharie, D., Stefanescu, C., Hébuterne, X., Abitbol, V., Nachury, M., Brixi, H., Bourreille, A., Picon, L., et al. (2018). Efficacy of adalimumab in patients with Crohn's disease and symptomatic small bowel stricture: a multicentre, prospective, observational cohort (CREOLE) study. *Gut* 67, 53–60. <https://doi.org/10.1136/gutjnl-2016-312581>.
39. Gong, W., Zheng, T., Guo, K., Fang, M., Xie, H., Li, W., Tang, Q., Hong, Z., Ren, H., Gu, G., et al. (2020). Mincle/Syk Signalling Promotes Intestinal Mucosal Inflammation Through Induction of Macrophage Pyroptosis in Crohn's Disease. *J. Crohns Colitis* 14, 1734–1747. <https://doi.org/10.1093/ecco-jcc/jjaa088>.

STAR★METHODS

KEY RESOURCES TABLE

| REAGENT or RESOURCE | SOURCE | IDENTIFIER |
|---|---------------------------|---|
| Antibodies | | |
| anti-MerTK antibody | Abcam | Cat#ab52968 |
| anti-MerTK antibody for LC-MS | Abcam | Cat#ab300136 |
| anti-Phospho-MerTK antibody | Fab Gennix | Cat#PMKT-140AP |
| anti-COL1A1 antibody | Servicebio | Cat#GB11022-3 |
| anti-CLO3A1 antibody | Servicebio | Cat#GB111629 |
| anti-CD206 antibody | Servicebio | Cat#GB113497 |
| anti-OPN antibody | R&D systems | Cat#AF808-SP |
| anti-OPN antibody | Servicebio | Cat#GB11500 |
| anti-cleaved caspase 3 antibody | Abcolonal | Cat#a19654 |
| anti-caspase 3 antibody | Abcam | Cat#ab32150 |
| anti-tgf-beta1 antibody | Abcolonal | Cat#a2124 |
| anti-Phospho-p44/42 MAPK (Erk1/2) antibody | Cell Signaling Technology | Cat#4370T |
| anti-ERK1/2 antibody | Abcam | Cat#ab184699 |
| anti-tubulin antibody | Proteintech | Cat#11224-1-AP |
| anti-GAPDH antibody | Cell Signaling Technology | Cat#5174s |
| anti-mouse IgG, HRP-linked antibody | Cell Signaling Technology | Cat#7076 |
| anti-rabbit IgG, horseradish peroxidase (HRP)-linked antibody | Cell Signaling Technology | Cat#7074 |
| HRP-conjugated donkey anti-goat IgG (H+L) | Servicebio | Cat#GB23404 |
| Biological samples | | |
| PBMCs | Human peripheral blood | N/A |
| Human colon tissue | Human participants | N/A |
| BMDMs | Mice bone marrow | N/A |
| Chemicals, peptides, and recombinant proteins | | |
| Mouse GAS6 protein | R&D systems | Cat#AF-986 |
| Human Gas6 protein | R&D systems | Cat#986-GS-025 |
| Deposited data | | |
| LC-MS raw data | This paper | lprox: IPX0008922000 |
| Experimental models: Cell lines | | |
| NCM460 | Jiangsu KeyGEN BioTECH | Cat#KGG3113-1 |
| RAW264.7 | Jiangsu KeyGEN BioTECH | Cat#KGG2201-1 |
| L929 | Jiangsu KeyGEN BioTECH | Cat#KGG1306-1 |
| CT26 | Jiangsu KeyGEN BioTECH | Cat#KGG2229-1 |
| Experimental models: Organisms/strains | | |
| Mice | Cyagen Biosciences | C57BL/6 |
| Oligonucleotides | | |
| See Table S2 for primers sequence. | This paper | N/A |
| Software and algorithms | | |
| GraphPad Prism version 9.0 | GraphPad Software | Prism 9: Taking your analyses and graphs to higher dimensions (graphpad.com) |
| ImageJ software | ImageJ | RRID: SCR_003070 |
| Microsoft Office 2021 | Microsoft Windows | N/A |

RESOURCE AVAILABILITY

Lead contact

Further information and requests for resources and reagents should be directed to and will be Dr. Jianan Ren (jiananr@nju.edu.cn).

Materials availability

This study did not generate new unique reagents.

Data and code availability

- Data: The data presented in this study are available in the article and [supplemental information](#).
- Code: LC-MS raw data in this paper could be accessed in iprox (accession code: IPX0008922000).
- Any additional information required to re-analyse the data reported in this paper is available from the [lead contact](#) upon request.

EXPERIMENTAL MODEL AND STUDY PARTICIPANT DETAILS

Ethical approval for human and animal studies

This study was performed in accordance with the Declaration of Helsinki. All human and animal tissue samples used in this study were purchased from a licensed tissue bank. Letter of approval is available on request. Collection of tissue samples for this study was approved as part of the study protocol. This study was approved by the Institutional Review Board at Jinling Hospital. All adult participants provided written informed consent to participate in this study.

Ethical approval number for human and animal participants: human: 2023DZSKT-180; Animal:2021DZGKJDWLS-00104.

Human sample collection and analysis

The collection of human specimens taken during bowel resection surgery from CD patients, as well as the collection of non-inflamed, non-stenotic controls, was approved by the Institutional Review Board at Jinling Hospital. Each participant provided written informed consent. More details on patients can be found in [Table S1](#). Preoperative gastrointestinal radiography determined the obstruction symptoms and regions, and longitudinal ulcers and markedly thickened intestinal wall were confirmed through intraoperative biopsy specimen observation by the surgeon. Representative Masson-trichrome staining confirmed the increased deposition of collagen in the stenotic intestine. Histology in HE staining showing tissue destruction and presence of massive inflammatory cells would be used to justify the selection of inflammatory tissue. Inflamed samples were provided by inflamed CD patients (Montreal B1), while fibrotic samples were provided by stricturing CD patients (Montreal B2). The assessment of disease phenotype (The Montreal classification) is based on a comprehensive analysis of clinical manifestations and surgical pathology specimens.

Peripheral blood (4 ml) was collected from CD patients. Peripheral blood mononuclear cells (PBMCs) were isolated by a human lymphocyte separation medium (KGA830; KeyGEN BioTECH), centrifuged at 1500rpm for 20-30min, and washed twice with PBS. Next, monocytes were resuspended (10^6 /ml) in complete RPMI1640 medium (KGM31800N-500; KeyGEN BioTECH), seeded into a 6-well plate, and cultured for 7 days in a 5% CO₂ incubator at 37°C. On Day 0 and 4, macrophages were stimulated with 10 ng/ml granulocyte-macrophage colony-stimulating factor (GM-CSF, HY-P7016A; MedChemExpress).

Mice

Male C57BL6/J mice were purchased from the Model Animal Research Center of Nanjing University and obtained from Cyagen Biosciences. All mice were housed in individually ventilated cages and age-matched 6–8-week-old male mice (4-6 weeks old mice were needed for extracting bone-marrow-derived macrophages) were used in all experiments. Animal care and use were approved by Jinling Hospital Animal Care Committee.

Experimental models of chronic colitis

Chronic inflammation was induced by 3 cycles of 7 days of 2% (w/vol) dextran sodium salt (DSS, MW 36,000–50,000; MP Biomedicals) in drinking water followed by 2 weeks of tap water. Fibrotic mouse model would be evaluated by histologic fibrosis score. The model of acute colitis was induced with 7 days of 3% DSS in drinking water. Colitis model would be evaluated by Mayo DAI (Disease Activity Index) score. The mice were killed on day 8 in the acute model and day 64 in the chronic model. Mice were randomized into groups. In selected experiments, mice were treated daily from day 0/21/42 by oral gavage with water or UNC2025 (Selleck Chemicals) at 3 mg/kg. The flow chart is shown in [Figure S2A](#).

METHOD DETAILS

Histology, immunohistochemistry, and immunofluorescence

For histological evaluation, fresh human intestinal mucosal specimens and colon tissues from animals were fixed with 4% paraformaldehyde, dehydrated in ethanol, embedded in paraffin, and stained with hematoxylin–eosin (H&E) under standard conditions. For Masson's trichrome

staining, the paraffin sections were stained with Weigert's cassiocarpa semen and Masson dye. For immunohistochemical staining, the paraffin sections were deparaffinized in xylene, rehydrated in a concentration gradient of ethanol, subjected to antigen retrieval, followed by incubation with primary and secondary antibodies, and visualized with the DAB substrate kit. Finally, the sections were counterstained with Mayer's hematoxylin, rinsed with water, differentiated by alcohol, dehydrated, cleared, and mounted. Primary antibodies for staining of human intestinal mucosa were against MerTK (ab52968; Abcam), COL1A1 (GB11022-3; Servicebio), COL3A1 (GB111629; Servicebio), CD206 (GB113497; Servicebio), OPN (GB11500; Servicebio) and cleaved caspase 3 (GB11532; Servicebio). Primary antibodies for staining of mouse colon tissues were against MerTK (ab184086; Abcam), COL1A1 (GB11022-3; Servicebio), and COL3A1 (GB111629; Servicebio).

For immunofluorescent staining, cultured cells were fixed with 4% paraformaldehyde, followed by incubation with 2% bovine serum albumin plus 1% newborn bovine serum in PBS for 60 min at room temperature to block the nonspecific background. Human tissues were incubated at 4°C overnight with primary antibody to OPN (Cat# AF808-SP, R&D systems). A confocal scanning microscope (FV1000; Olympus Corporation) was used for imaging analysis.

Cell culture and transfection

RAW 264.7 (Abelson murine leukemia virus-induced tumor cell line), CT26 (murine colon cancer cell line), L929 (murine fibrosarcoma L929 cell line), and NCM460 (normal human colon mucosal epithelial cell line) were purchased from Jiangsu KeyGEN BioTECH and cultured in Dulbecco's modified Eagle's medium (DMEM)-F12 (KGM12500N-500; KeyGEN BioTECH) or RPMI-1640 medium (KGM31800N-500; KeyGEN BioTECH) with 10% fetal bovine serum (10100147C; Gibco) and 1% penicillin/streptomycin (15140163; Gibco). For siRNA or plasmid transient transfection, cells were seeded in 6-well plates until they reached 40–60% confluence and then transfected with the expression vectors or specific siRNAs targeting OPN or MerTK using Lipofectamine 3000 Transfection Reagent (L3000150; Thermo Fisher Scientific). Sequence construction was provided by General Biology. After 6 hours, the starved medium was changed with complete DMEM, and cell protein samples were extracted after 60 hours, or RNA samples after 48 hours.

Generation of apoptotic cells

Human NCM460 and mouse CT26 cells were exposed to UV irradiation at 254 nm for 15 minutes, 30 minutes, 1 hour, or 2 hours, and cultured in a CO₂ incubator for 2 hours before performing experiments. After 2 hours, we collected the supernatant and digested the cells, and counted the cells after centrifugal resuspension. The apoptotic cells were resuspended in complete DMEM at 2×10^6 cells/mL. Apoptotic cells were cocultured with human macrophages (differentiated from PBMCs) or RAW264.7 cells for 45 minutes.

ELISA

Cell supernatant was collected and analyzed by the Mouse/Rat TGF- β 1 ELISA Kit (PT878; Beyotime).

Quantitative real-time PCR

The mRNA levels were measured using quantitative real-time (q)PCR as previously described.³⁹ After total RNA was extracted with TRIzol reagent (Invitrogen), it was reverse-transcribed with HiScript® III RT SuperMix for qPCR (+gDNA wiper) (#R323; Vazyme). For real-time PCR, use 1 μ L template in a 10- μ L reaction containing 1.0 μ L each primer and 5 μ L ChamQ Universal SYBR qPCR Master Mix (#Q711; Vazyme). Primers are shown in Table S2 (mentioned in Table S2). Results were normalized using β -actin gene expression and shown as the relative expression value.

Western blotting

Primary antibodies were: MerTK (ab52968 for humans, ab184086 for mice; Abcam), Phospho-MerTK (PMKT-140AP; Fab Gennix), OPN (ab214050 for humans; Abcam; AF808-SP for mice; R&D Systems), TGF- β 1 (A2124; Abclonal), Phospho-p44/42 MAPK (Erk1/2) (4370T; Cell Signaling Technology), ERK1/2 (ab184699; Abcam), caspase 3 (ab32150; Abcam), cleaved caspase 3 (a19654; Abcolonal), Tubulin (11224-1-AP; Proteintech), GAPDH (#5174S; Cell Signaling Technology). Secondary antibodies were: anti-mouse IgG, HRP-linked antibody (#7076; Cell Signaling Technology), anti-rabbit IgG, horseradish peroxidase (HRP)-linked antibody (#7074; Cell Signaling Technology), HRP-conjugated donkey anti-goat IgG (H+L) (GB23404; Servicebio). Western blotting was performed as previously described.³⁹ Extracted protein samples were separated by 8% SDS-PAGE and transferred to a polyvinylidene fluoride membrane. After incubation with the primary antibodies for 16 hours and washing the membrane, the samples were incubated with secondary antibodies. Immunoreactive bands were visualized on a Tanon-5200 Chemiluminescent Imaging System (Tanon Science & Technology).

Wound healing assay

L929 cells were seeded in 6-well plates for 18 hours. Subsequently, cells were washed twice with PBS and incubated with a starvation medium from the supernatant of RAW264.7 culture. We used a 200- μ L sterile pipette tip to create a scratch under sterile conditions and migration of cells into the gap generated was observed. Images of the gap were captured at 0, 6, 20, 24, and 48 hours under a confocal scanning microscope. The quantification was performed with ImageJ software (version 1.8.0, National Institutes of Health).

LC-MS analysis

Use liquid chromatography and mass spectrometry (LC-MS) to identify the proteins directly interacting with MerTK in RAW 264.7 cells. After collecting all proteins bound to MerTK by immunoprecipitation, the samples were subjected to LC-MS analysis. The data were acquired with an LC-MS system (LTQ Orbitrap Elite System, analyzed by APTBIO). The detailed protocol is as follows:

Filter-aided Sample preparation (FASP)

Mix 30 μ L protein with DTT to a final concentration of 100mM DTT. Incubate at 95°C for 5 min and cool to room temperature. Add 200 μ L UA buffer (8M Urea, 150mM Tris-HCl pH8.5), mix and transfer to a 10kDa centrifugal filter unit. Centrifuge at 14000g for 30 minutes and discard the flow-through. Add 200 μ L UA buffer (8M Urea, 150mM Tris-HCl pH8.5) to the filter unit and mix. Centrifuge at 14000g for 30 minutes and discard the flow-through. Add 100 μ L IAA(100mM IAA in UA) to the filter unit and incubate at room temperature in dark for 30 minutes. Centrifuge at 14000g for 30 minutes and discard the flow-through. Add 100 μ L UA buffer (8M Urea, 150mM Tris-HCl pH8.5) to the filter unit and mix. Centrifuge at 14000g for 30 minutes and discard the flow-through. Add 100 μ L 2mM NH_4HCO_3 to the filter unit and mix. Centrifuge and discard the flow-through. Add 48 μ L Trypsin buffer to the filter unit and spin at 600rpm for 1 minute. Incubate at 37°C for 16-18 hours. Collect the flow-through and determine the concentration of trypsin-digested peptides by UV spectrometry at 280 nm.

High Performance Liquid Chromatography (HPLC)

Separating peptides of each sample by using Easy nLC system (Thermo Scientific). The Peptides were loaded in 95% solvent A (0.1% formic acid) on a two-column set-up consisting of a trap column (Thermo Scientific Acclaim PepMap100, 100 μ m*2cm, nanoViper C18) and an analytical column (Thermo scientific EASY column, 15cm, ID150 μ m, 3 μ m, C18). A gradient of solvent B (84% acetonitrile and 0.1% Formic acid) was applied at a flow rate of 300 nL/min as follows: 0% to 60% B in 50 min; 60% to 90% B in 4 min; and 90% B in 6 min.

Mass spectrometry assay

Eluted peptides were analyzed using the Q-Exactive mass spectrometer (Thermo Scientific) for 60 min. The mass spectrometer was operated in positive ion mode. Full scan MS spectra (m/z 300–1800) were acquired with a resolution of 70000 at 100 m/z. Automatic gain control (AGC) target was set to 1e6; Maximum inject time was 50 ms, and dynamic exclusion was 30.0s. Up to 20 most intense ions were selected for higher-energy collisional dissociation fragmentation depending on signal intensity. Isolation window was 1.5m/z; MS/MS fragment spectra were acquired with a resolution of 17500 at 100 m/z, AGC target was 1e5; Maximum inject time was 50 ms; Normalized collision energy was 27eV and underfill was 0.1%.

QUANTIFICATION AND STATISTICAL ANALYSIS

Statistical analysis was performed using GraphPad Prism version 9.0. Statistical analysis to compare the mean values for multiple groups was performed using GraphPad Prism by one- or two-way ANOVA with Bonferroni's multiple-comparisons test. Student's *t*-test or one-way ANOVA was used to determine significance. All of the statistical details of experiments, including the statistical tests used and the exact value of sample sizes, can be found in the figure legends. All error bars represent SEM. A difference of $P < 0.05$ was considered statistically significant (* $P < 0.05$; ** $P < 0.01$; *** $P < 0.001$; **** $P < 0.0001$).